

CHEMISTRY OF MATERIALS

VOLUME 19, NUMBER 7

APRIL 3, 2007

© Copyright 2007 by the American Chemical Society

Communications

Facile Route to Aligned One-Dimensional Arrays of Colloidal Nanoparticles

Changdeuck Bae,[†] Hyunjung Shin,^{*,†} and Jooho Moon[‡]

School of Advanced Materials Engineering, Kookmin University, Seoul 136-702, Korea, and Department of Materials Science and Engineering, Yonsei University, Seoul 120-749, Korea

Received September 2, 2006

Revised Manuscript Received January 8, 2007

This communication describes a new approach to the self-assembly of nanoparticles into aligned, single arrays. The proposed approach uses no physical nanopatterns with a width of the diameter of nanoparticles, which are normally used to trap the particles into single arrays. Instead, a facile route is utilized in which 1D arrays of submicrometer-sized nanoparticles are reproducibly formed along the step edges of micrometer-scale stripe patterns in a large area. It is proposed that such structures form by a previously unknown growth mechanism resulting from a shadow effect generated under a controlled convective flow of the colloidal particle suspension.

In the past several years, various methods for preparing aligned 1D arrays of nanomaterials have been reported.^{1,2}

Although those methods can be categorized into template-assisted self-assembly, convective assembly, and spin-casting, in accordance with the formation means, they commonly require surface nanotemplates. The nanotemplates are either physical trenches or chemical patterns in which the particles are geometrically fitted into the templates forming single arrays. For example, aligned 1D arrays of micrometer-scale spheres are generated within photolithographically defined micrometer scale stripe patterns, whereas single arrays of nanoparticles are formed in nanotrenches prepared by means of nanolithographic techniques.^{1(a,b)} In this study, for the first time, a new phenomenon is reported in which colloidal submicrometer particles are self-assembled in a line along each step edge of micrometer-scale stripe patterns without the need for nanolithographic techniques. The growth of the aligned colloidal arrays is explained in terms of a shadow effect and rearrangement by lateral capillary forces under the controlled convective flow of the colloidal suspension over the underlying patterns.

Monodisperse silica spheres 200–800 nm in diameter were synthesized through the modified Stöber method³ and prepared by suspension in a controlled aqueous solution⁴. A drying cell that can physically confine the suspension was constructed: Stripe patterns of SiO₂ (100 nm) films ~3 μm wide and spaced at ~3 μm were fabricated by conventional photolithography, followed by wet chemical etching onto a silicon substrate. Following this, a millimeter-scale cylindrical polymer tube was glued onto the patterned substrate. The concentration and the quantity of the suspension were

(3) Stöber, W.; Berner, A.; Blaschke, R. *J. Colloid Interface Sci.* **1969**, *29*, 710.

(4) The optimum solvent and its volume ratio were a 1:1 mixture of water and ethanol. These conditions were used to maintain a constant drying rate in ambient conditions in place of control over the humidity in a chamber.

* Corresponding author. E-mail: hjshin@kookmin.ac.kr.

[†] Kookmin University.

[‡] Yonsei University.

- (1) (a) Yin, Y.; Lu, Y.; Gates, B.; Xia, Y. *J. Am. Chem. Soc.* **2001**, *123*, 8718. (b) Xia, Y.; Yin, Y.; Lu, Y.; McLellan, J. *Adv. Funct. Mater.* **2003**, *13*, 907. (c) Cui, Y.; Bjork, M. T.; Liddle, J. A.; Sonnichsen, C.; Boussett, B.; Alivisatos, A. P. *Nano Lett.* **2004**, *4*, 1093. (d) Xia, D.; Brueck, S. R. J. *Nano Lett.* **2004**, *4*, 1295. (e) Xia, D.; Biswas, A.; Li, D.; Brueck, S. R. J. *Adv. Mater.* **2004**, *16*, 1427.
- (2) (a) Masuda, Y.; Itoh, M.; Yonezawa, T.; Koumoto, K. *Langmuir* **2002**, *18*, 4155. (b) Chen, K. M.; Jiang, X.; Kimerling, L. C.; Hammond, P. T. *Langmuir* **2000**, *16*, 7825.

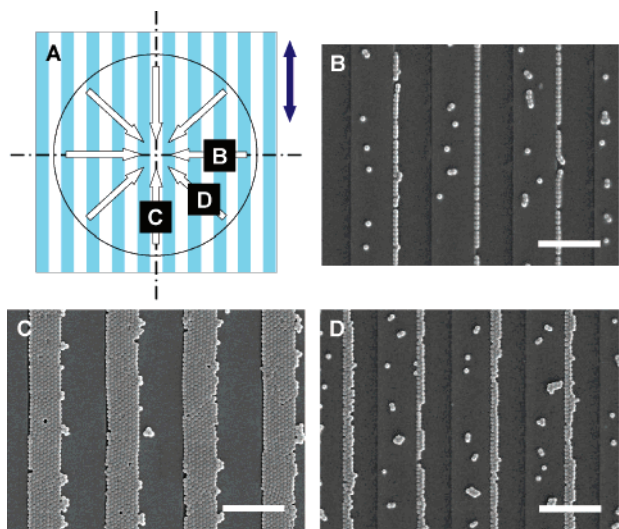


Figure 1. Case in which a cylindrical drying cell is used. (A) Schematic illustration of the cell. The solid circle displays the wall of the cell. The blue arrow indicates the direction of the underlying stripe patterns. The empty arrows indicate the direction of convective flow. (B–D) FE-SEM images obtained around Regions B, C, and D in Figure 1A, respectively. All scale bars correspond to $5 \mu\text{m}$.

calculated to cover the surface in the cell with a monolayer of spheres. Typically, a droplet of $5 \mu\text{L}$ of a 0.5 wt % suspension of silica particles was placed at the center of the surface of the cell using a micropipette and allowed to dry in ambient conditions⁵ for ~ 1 h. After the solvents were dried, the cylindrical cell was removed from the substrate. The resulting arrays on the surfaces were observed by field-emission scanning electron microscopy (FE-SEM).

Figure 1 shows representative images of the resulting arrays at three different positions on the surface of the circular cell. Depending on the location, lines with different widths of colloidal particles were observed. It was found that the width of the lines ranges from micrometer-scale stripes to single arrays, consistent with the angle between the moving direction of the drying front and the direction of the underlying stripes. In the present system, as the solvent evaporates from the curved air–liquid interface at the center of the surface of the substrate in the cell, a circular-shaped three-phase contact line forms and the contact line subsequently recedes from the center to the wall of the cell as the drying proceeds. Because of the higher drying rate of the solvent at the drying front compared to any other interfaces, there must be a continuous radial inward flow of the solvent from the wall of the cell to the contact line to compensate for the liquid removed by evaporation. This convective flow and the suspended particles it carries are responsible for the particle accumulation around the contact line.^{6,7} For example, at Region B, as shown in Figure 1A, the direction of the

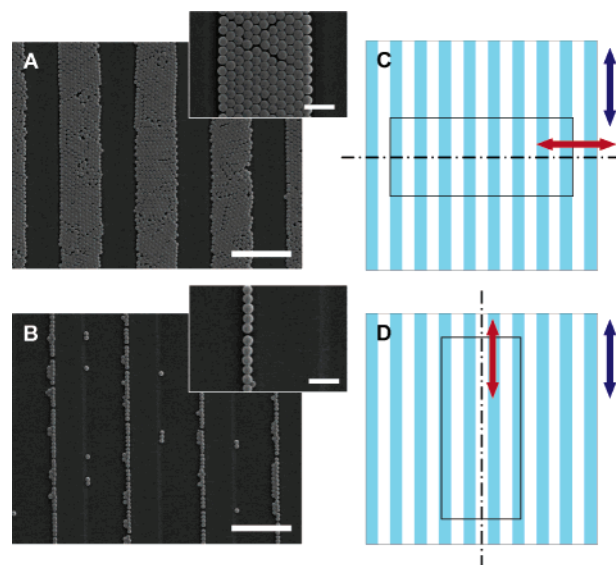


Figure 2. Case in which a rectangular drying cell is used. (A) and (B) FE-SEM images obtained from the set-ups of (C) and (D), respectively. In both (C) and (D), the solid rectangles display the wall of the cells; the red arrows indicate the direction of the rectangular cells and the blue arrows indicate the direction of the underlying stripe patterns. The scale bars correspond to $5 \mu\text{m}$ for the low-magnification images and $1 \mu\text{m}$ for the insets.

particle flux is generally perpendicular with respect to the underlying stripe patterns, and the particles form single arrays of spheres (Figure 1B). At Region C, the direction of the flux is parallel with the stripes, and the particles are completely filled up to form 2D crystals between the stripes (Figure 1C); at Region D, the flux crosses with an angle of $\sim 45^\circ$ and the particles form colloidal patterns with 2–3 colloidal arrays (Figure 1D). A number of particles and clusters on the top surface of the SiO_2 stripe patterns were observed. Such a pinning effect can be prevented by controlling the wettability of the surfaces.^{8,9}

The experiments above were carried out with a circular-shaped cell in which various directions of the particle flux coexist, with respect to the direction of the line patterns. To show that the formation of single arrays indeed resulted from the relationship between the directions of the flux and the pattern, a rectangular tube was used instead of a cylindrical tube. The rectangular tube can generate the particle flux in virtually one direction with respect to the stripe patterns. Two drying cells were prepared with rectangular tubes on patterned SiO_2 films: one perpendicular to the stripes (Figure 2C) and the other parallel (Figure 2D). Before attaching the tubes, the substrates were treated with piranha solutions to render them hydrophilic. In the parallel case, the particles

(5) Typically, room temperature and $\sim 50\%$ relative humidity.

(6) (a) Denkov, N. D.; Velev, O. D.; Kralchevsky, P. A.; Ivanov, I. B.; Yoshimura, H.; Nagayama, K. *Langmuir* **1992**, *8*, 3183. (b) Denkov, N. D.; Velev, O. D.; Kralchevsky, P. A.; Ivanov, I. B.; Yoshimura, H.; Nagayama, K. *Nature* **1993**, *361*, 26.

(7) (a) Kralchevsky, P. A.; Nagayama, K. *Langmuir* **1994**, *10*, 23. (b) Kralchevsky, P. A.; Denkov, N. D.; Paunov, V. N.; Velev, O. D.; Ivanov, I. B.; Yoshimura, H.; Nagayama, K. *J. Phys.: Condens. Mater.* **1994**, *6*, A395. (c) Kralchevsky, P. A.; Denkov, N. D. *Curr. Opin. Colloid Interface Sci.* **2001**, *6*, 383. (d) Yamaki, M.; Higo, J.; Nagayama, K. *Langmuir* **1995**, *11*, 2975.

(8) We tried to achieve clear arrays without any pinned particles on the top of the stripes through surface treatments, and the results are shown in panels A and B of Figure 2.

(9) Ko, H.-Y.; Park, J.; Shin, H.; Moon, J. *Chem. Mater.* **2004**, *16*, 4212.

(10) Note that there are no particles or clusters sitting on top of the surfaces of the SiO_2 stripes, as shown in panels A and B of Figure 2. We suspect that such clear arrays of colloidal spheres result from the rapid thinning of the liquid film on the hydrophilic surfaces with a contact angle of $\sim 0^\circ$. In accordance with the growth mechanism of colloidal 2D crystals, aggregation of the particles begins at the thickness of the liquid nearly equal to the diameter of the sphere. That is, the thin wetting films of the solvent as a result of the surface treatment provides a relatively short incubation time in the formation of aggregates of particles on the stripes.

form a pattern of 2D colloidal crystals between the SiO₂ stripes (Figure 2A) as expected from template-assisted experiments by other researchers.¹ In the perpendicular case, in contrast, the particles form aligned single arrays along each side of the stripes in a relatively large area (Figure 2B).¹⁰ In this case, compared with Figure 2A, we found that the rest of the particles from the droplet have accumulated around the wall of the cell, as observed for 2D convective assembly in the confined cell.^{6(a)} An ~ 0.01 mm² area for the single arrays was observed in this study. With the appropriate design of a drying cell, however, there is no reason that these arrays cannot be achieved over a large area, implying that aligned single arrays of nanomaterials can be fabricated without the use of expensive and/or sophisticated nanolithographic techniques.

Although the mechanisms of the 2D crystal growth of particles on both flat surfaces and templates are well-known, they are insufficient for an understanding of the formation of single arrays in the present experiments. For the ordering process of colloidal silica particles between SiO₂ stripe patterns, the mechanism is similar to the growth of 2D crystals formed by spheres on flat surfaces but differs in that the nucleation and growth of colloids occur between the stripe patterns. During the solvent drying process, the presence of the stripe trenches gives rise to the difference in the receding velocity of the three-phase contact line between the trench and the stripe. That is, the wetted liquid films in the trenches can stay longer there compared to the surface of the stripe pattern. Therefore, if any colloids are deposited onto stripe surfaces, they are swept down into the trenches by the lateral capillary forces and contribute to the growth of the colloidal pattern.

The formation of 1D array structures consisting of colloidal spheres by a combination of both the convective flow and the crossing of the solid stripes can be explained as follows: When the solvent influx carries the suspended spheres to the three-phase contact line, the presence of the stripe patterns results in a shadow effect;^{11,12} the coupling between the hydrodynamics and electrostatic repulsion creates regions of the particle absence, the so-called shadow zone, at one-side of the stripe patterns. Electrostatic repulsion between the two silica surfaces of the particles and the relief patterns prohibits low-level flying of the particles over the surfaces of the substrate, competing with the shear components in the velocity of the z-axis for the flow that determines the resulting trajectory of the particles, as depicted in Figure 3. Consequently, the opposite side of the step edge of the stripe pattern rather than the shadow zone side is favored for the formation of colloidal arrays. Even if some particles are deposited on the trench surface slightly away from the side of the stripe patterns and rejected for the single-array formation, the particles can join into a single array. They can move into the step edge via lateral capillary forces

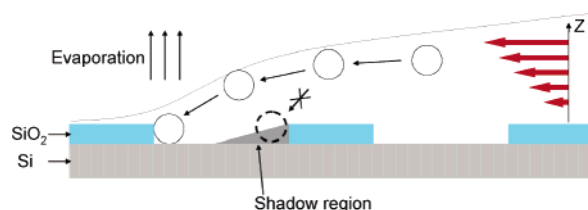


Figure 3. Schematic illustration of the shadow effect. When the suspended particles deposit around the contact line, the coupling between the hydrodynamics and electrostatic repulsion creates regions of particle absences, the so-called shadow zone; electrostatic repulsion between the particles and the relief patterns and shear components in the velocity of the z-axis for the flow direct these effects. The red arrows indicate the shear components in the velocity for the flow.

between the particle pinned in the middle of the trench surfaces and the side of the stripe generating the aligned single arrays.^{13,14}

A new finding in which aligned particle arrays can be fabricated on physically patterned micrometer-scale surfaces is reported. This is possible by combining the convective transport direction of colloidal suspensions and the underlying pattern direction. The direction of the influx of the suspension over the underlying patterns was shown to account for the width of colloidal stripes through two different experiments using rectangular cells. The formation of aligned colloidal arrays is explained in terms of a shadow effect and the rearrangement of capillary force-driven particles. It is anticipated that this strategy for self-assembly into aligned 1D arrays can serve in the preparation of aligned arrays of other nanomaterials such as rods, tubes, or wires as well as metal colloids, which have potential in photonic¹⁵ as well as plasmonic¹⁶ applications.

Acknowledgment. This work was supported by a grant (R01-2002-000-00318-0) from the Korean Science and Engineering Foundation (KOSEF). J.M. thanks the program of the National Research Laboratory of the Korean Ministry of Science and Technology (MOST). H.S. also thanks the Center for Nanostructured Materials Technology of MOST (M105K0010026-06K1501-02610) under the 21st Century Frontier R&D Programs of MOST and the Center for Materials and Processes of Self-assembly (R11-2005-048-00000-0) by the Engineering Research Center Program of MOST/KOSEF. This work was also supported by the research program 2005 of Kookmin University, Korea. C.B. has been partially supported by the Seoul Science Fellowship Program of Seoul City, Korea.

CM062081P

(11) Ye, Y.-H.; Badilescu, S.; Truong, V.-V.; Rochon, P.; Natansohn, A. *Appl. Phys. Lett.* **2001**, *79*, 872.

(12) Ko, C.-H.; Elimelech, M. *Environ. Sci. Technol.* **2000**, *34*, 3681.

(13) Dushkin, C. D.; Kralchevsky, P. A.; Yoshimura, H.; Nagayama, K. *Phys. Rev. Lett.* **1995**, *75*, 3454.

(14) Aizenberg, J.; Braun, P.; Wiltzius, P. *Phys. Rev. Lett.* **2000**, *84*, 2997.

(15) (a) Yablonovitch, E. *Phys. Rev. Lett.* **1987**, *58*, 2059. (b) John, S. *Phys. Rev. Lett.* **1987**, *58*, 2486. (c) Joannopoulos, J. D.; Villeneuve, P. R.; Fan, S. *Nature* **1997**, *386*, 143. (d) Joannopoulos, J. D. *Nature* **2001**, *414*, 257.

(16) (a) Maier, S. A.; Kik, P. G.; Atwater, H. A.; Meltzer, S.; Harel, E.; Koel, B. E.; Requicha, A. A. G. *Nat. Mater.* **2003**, *2*, 229. (b) Maier, S. A.; Brongersma, M. L.; Kik, P. G.; Meltzer, S.; Requicha, A. A. G.; Koel, B. E.; Atwater, H. A. *Adv. Mater.* **2001**, *13*, 1501. (c) Abdolvand, A.; Podlipensky, A.; Matthias, S.; Syrowatka, F.; Gösele, U.; Seifert, G.; Graener, H. *Adv. Mater.* **2005**, *17*, 2983.